Three-Dimensional Salphen-Based Covalent Organic Frameworks as Catalytic Antioxidants

Shichen Yan, Xinyu Guan, Hui Li, Daohao Li, Ming Xue, Yushan Yan, Valentin Valtchev, Shilun Qiu, Qianrong Fang

Three-Dimensional Salphen-Based Covalent Organic Frameworks as Catalytic Antioxidants

Shichen Yan,[†] Xinyu Guan,[†] Hui Li,[†] Daohao Li,[†] Ming Xue,[†] Yushan Yan,[‡] Valentin Valtchev,[†,‖] Shilun Qiu[†] and Qianrong Fang[*,†]

[†]State Key Laboratory of Inorganic Synthesis and Preparative Chemistry, Jilin University, Changchun 130012, P. R. China

[‡]Department of Chemical and Biomolecular Engineering, Center for Catalytic Science and Technology, University of Delaware, Newark, DE 19716, USA

[‖]Normandie Univ, ENSICAEN, UNICAEN, CNRS, Laboratoire Catalyse et Spectrochimie, 6 Marechal Juin, 14050 Caen, France

Supporting Information Placeholder

ABSTRACT: The development of three-dimensional (3D) functionalized covalent organic frameworks (COFs) is of critical importance for expanding their potential applications. However, the introduction of functional groups in 3D COFs remains largely unexplored. Herein we report the first example of 3D Salphen-based COFs (3D-Salphen-COFs) and their metal-containing counterparts (3D-M-Salphen-COFs), the later being further used as catalytic antioxidants. These Salphen-based COFs exhibit high crystallinity and specific surface area in addition to excellent chemical stability. Furthermore, the Cu(II)-Salphen COF displayed high activity in the removal of superoxide radicals. This study not only presents a new pathway to construct 3D functionalized COFs, but also promotes their applications in biology and medicine.

Covalent organic frameworks (COFs), an emerging class of crystalline porous materials, are composed of pure organic skeletons connected by strong organic bonds.[1-5]. Since the pioneering work of Yaghi in 2005, various COFs with different backbones and functional groups have been synthesized and employed as platforms for applications such as gas adsorption and separation,[6-8] optoelectronics,[9,10] heterogeneous catalysis,[11-13] and a number of others.[14-20] Yet most of the reported COFs are two-dimensional (2D) frameworks with eclipsed stacking structures.[21,22] Three-dimensional (3D) COFs have recently attracted much attention due to their unique porous structures and outstanding performances.[23-28] We have reported a series of 3D COFs by the meticulous design of building units, including 3D ionic COFs for selective ion exchange,[29] 3D ionic liquid containing COFs with high gas separation ability,[30] 3D carboxy-functionalized COFs for selective extraction of lanthanide ions,[31] and so on.[32-34] It must be noted, however, that 3D COFs are still limited so far, and thus the development of 3D COFs, especially 3D functionalized COFs, is important for improving their structural diversity and widening their potential applications.

Scheme 1. Strategy for preparing 3D-Salphen-COFs[a]

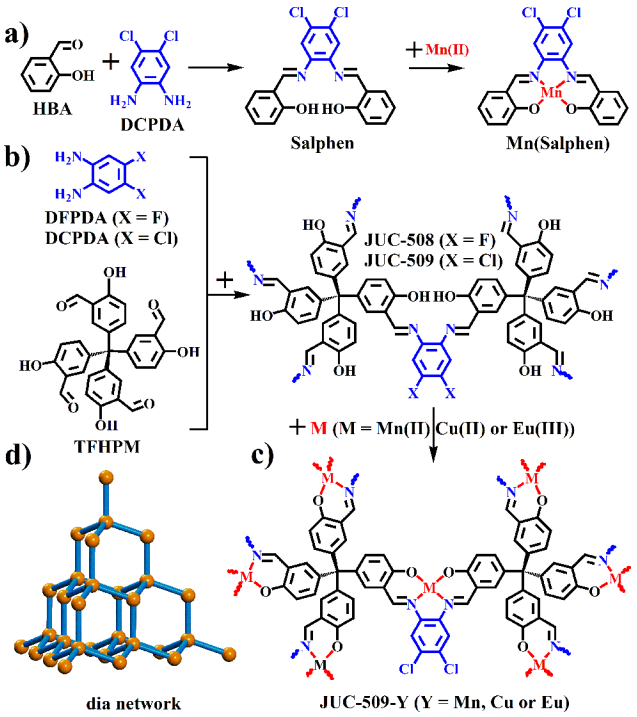

[a](a) The model reaction of Salphen unit and M-Salphen unit based on 2-hydroxybenzaldehyde (HBA) and 4,5-dichlorophenylene-1,2-diamine (DCPDA). (b) Condensation of tetrahedral tetrakis(3-formyl-4-hydroxylphenyl)methane (TFHPM) and two linkers containing diamine, 4,5-difluorophenylene-1,2-diamine (DFPDA) or DCPDA, to give novel 3D-Salphen-COFs, JUC-508 and JUC-509, respectively. (c) The preparation of 3D-M-Salphen-COFs, JUC-509-Y (Y = Mn, Cu or Eu), via the metal complexation. (d) The non-interpenetrated **dia** network in 3D-Salphen-COFs.

Herein, we addressed the above issues by designing 3D Salphen-based COFs (3D-Salphen-COFs) and their corresponding

metal-containing isostructures (3D-M-Salphen-COFs). The obtained COFs showed high crystallinity, open channels, good chemical stability, and large specific surface area. Furthermore, various metal ions (Cu(II), Mn(II) and Eu(III)) were successfully incorporated into the Salphen-based COFs, as the Cu(II)-Salphen COF exhibited the best performance in eliminating deleterious oxygen-derived free radicals. To the best of our knowledge, this study is the first case of 3D Salphen-based COFs and the application of COF materials as catalytic antioxidants.

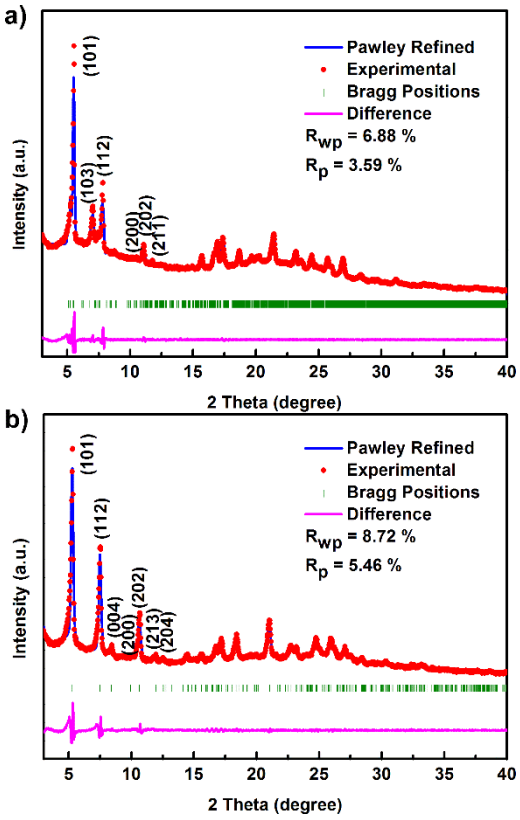

Figure 1. PXRD patterns of JUC-508 (a) and JUC-509 (b).

Our strategy for constructing 3D-Salphen-COFs embraces the form of both COF frameworks and Salphen units synchronously. As shown in Scheme 1a, 2-hydroxybenzaldehyde (HBA) and 4,5-dichlorophenylene-1,2-diamine (DCPDA) afford the model Salphen unit, which can be further assembled into Mn(II)-Salphen unit via the complexation (see the Supporting Information, SI, Section S1). On the basis of this reaction, we synthesized a tetrahedral salicylaldehyde-based monomer, tetrakis(3-formyl-4-hydroxylphenyl)methane (TFHPM). By the condensation of TFHPM and amino-based linkers, 4,5-difluorophenylene-1,2-diamine (DFPDA) or DCPDA, two extended 3D Salphen-based COFs, denoted as JUC-508 and JUC-509 respectively, can be obtained (Scheme 1b). Furthermore, JUC-509 can be gathered into 3D-M-Salphen-COFs by the introduction of Mn(II), Cu(II) or Eu(III) ions, denoted as JUC-509-Y (Y = Mn, Cu or Eu, Scheme 1c). Based on this design, TFHPM can be defined as a 4-connected node, and DFPDA or DCPDA can act as a 2-connected node, which results in the 3D network with the non-interpenetrated **dia** topology due to the steric effect of Salphen unit (Scheme 1d).[35]

Typically, 3D-Salphen-COFs were synthesized by suspending TFHPM with DFPDA or DCPDA in the mixed solvent of dioxane and mesitylene in the presence of acetic acid followed by heating at 120 °C for 3 days. Complementary characterizations have been employed for detailed structural definition of new materials. Scanning electron microscopy (SEM) and transmission electron microscopy (TEM) images of 3D-Salphen-COFs showed flower-like microstructure composed of prismatic several micrometers long crystals (Figures S1-S4). Peaks around 1616 cm^{-1} for JUC-508 and 1618 cm^{-1} for JUC-509 in Fourier transform infrared (FTIR) spectra indicated the formation of imine linkages, and the disappearance of peaks at 1658 cm^{-1} for both 3D-Salphen-COFs confirmed the complete transformation of aldehyde groups, which is similar to that from the model Salphen unit (Figures S5 and S6). The solid state ^{13}C cross-polarization magic-angle-spinning (CP/MAS) NMR spectra further confirmed the presence of carbon from the C=N bond at 163 ppm for JUC-508 and 161 ppm for JUC-509 (Figures S8 and S9). According to the thermogravimetric analysis (TGA), both 3D-Salphen-COFs are stable up to about 350 °C under nitrogen (Figures S10 and S11). Notably, their crystalline structures can be preserved in the aqueous solutions at pH = 1~14 (Figures S15 and S16).

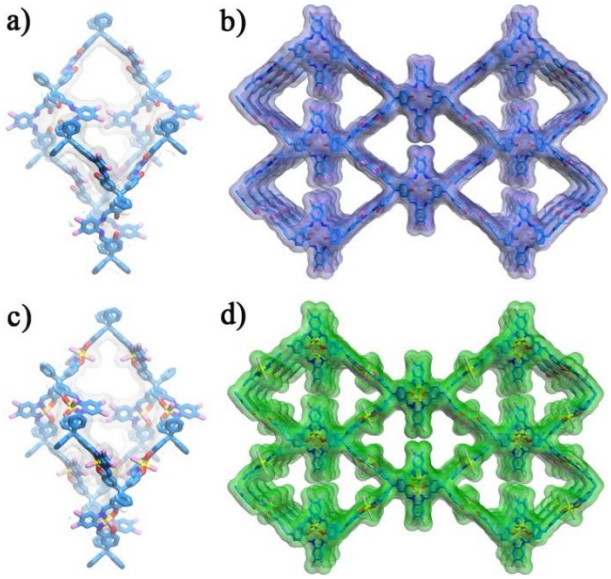

Figure 2. Structural representations of JUC-509 (a and b) and metal-containing JUC-509 (c and d).

The crystal structures of 3D-Salphen-COFs were resolved by the powder X-ray diffraction (PXRD) measurements in conjunction with structural simulations (Figure 1). After a geometrical energy minimization by using the Materials Studio software package[36] based on non-interpenetrated **dia** net for 3D-Salphen-COFs, the unit cell parameters were obtained (a = b = 19.153 Å, c = 41.988 Å and α = β = γ = 90° for JUC-508; a = b = 18.983 Å, c = 42.202 Å and α = β = γ = 90° for JUC-509). Furthermore, full profile pattern matching (Pawley) refinements were carried out on the experimental PXRD patterns. Peaks at 5.41, 7.19, 8.02, 10.31, 10.84 and 11.65° for JUC-508 correspond to the (101), (103), (112), (200), (202) and (211) Bragg peaks of space group *I*-42d (No. 122), respectively; peaks at 5.10, 7.80, 8.37, 9.31, 1021, 12.17 and 12.53° for JUC-509 correspond to the (101), (112), (004), (200), (202), (213) and (204) Bragg peaks of space group *I*-42d, respectively. The refinement results matched well with the observed patterns with good agreement factors ($R\omega p$ = 6.88% and Rp = 3.59% for JUC-508; $R\omega p$ = 8.72% and Rp = 5.46% for JUC-509). We also considered the alternative structures based on the 2-fold interpenetrated **dia** net from the same space group of *I*-42d for both 3D-Salen-COFs; however, their simulated patterns did not match to the experimental ones (Figures S17-20). On the basis of the above results, these Salphen COFs were proposed to have

the expected architectures with non-interpenetrated **dia** topology, which show microporous cavities with a diameter of about 1.2 nm (Figure 2 and Figure S21). Remarkably, almost all of 3D COFs with **dia** topology show multifold interpenetrated structures, and thus the successful preparation of 3D-Salphen-COFs with non-interpenetrated nets will benefit the development of 3D COFs with large pores.

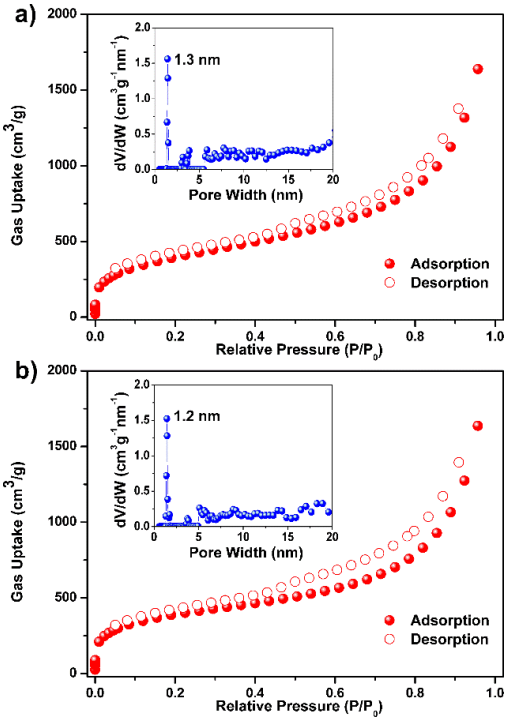

Figure 3. N_2 adsorption-desorption isotherms of JUC-508 (a) and JUC-509 (b). Inset: pore-size distribution calculated by fitting on the NLDFT model to the adsorption data.

The porosity and surface areas were measured by N_2 adsorption and desorption analysis (Figure 3). Both materials show a sharp uptake at a low pressure of $P/P_0 < 0.05$, which is characteristic of the microporous material. The inclination of isotherms in the 0.8-1.0 P/P_0 range and slight desorption hysteresis show the presence of textural mesopores, which is the consequence of the agglomeration of COF crystals.[34] The Brunauer-Emmett-Teller (BET) equation was applied over the $0.05 < P/P_0 < 0.30$ range of the isotherms, revealing BET surface areas of 1513 $m^2\ g^{-1}$ for JUC-508 and 1443 $m^2\ g^{-1}$ for JUC-509 (Figures S25 and S26). Pore size distributions of 3D-Salphen-COFs calculated by nonlocal density functional theory (NLDFT) showed pore with sizes of 1.3 nm for JUC-508 and 1.2 nm for JUC-509, respectively (Figure 3, inset), which is in good agreement with that of the proposed model (1.2 nm).

Encouraged by their high surface area and abundant Salphen units, a series of 3D-M-Salphen-COFs were subsequently acquired by immersing JUC-509 in a methanol solution of relative metal salts, giving JUC-509-Y (Y = Mn, Cu or Eu). The metal complexation of Salphen COFs could be easily visualized by their color change (Figure S28). Meanwhile, scanning electron microscope-energy dispersive X-ray spectra (SEM-EDS) analysis exhibited the uniform distribution of metal ions in the crystals (Figure S29). The ICP analysis of the resulting M-Salphen COFs showed that most of the Salphen pockets have been occupied by the metal ions (see Section S1 in SI). FTIR spectroscopy indicated the strong interaction between Salphen-COF and metal ions based on the shift of the IR bands for the imine groups from 1618 cm^{-1} (JUC-509) to 1608 cm^{-1} (JUC-509-Cu), 1606 cm^{-1} (JUC-509-Mn) or 1606 cm^{-1} (JUC-509-Eu), which is similar with the results from the model Salphen unit to Mn(II)-Salphen unit (from 1614 cm^{-1} to 1603 cm^{-1}, Figure S7). X-ray photoelectron spectroscopy (XPS) suggested Cu and Mn were in the +2 oxidtion state and Eu was in the +3 oxidation state (Figures S30-32). In addition, the retained PXRD patterns of 3D-M-Salphen-COFs pointed out that the crystalline structure was preserved after the metal incorporation (Figure 2 and Figures S22-24). The porosities were evaluated by N_2 adsorption and desorption analysis, which showed values slightly lower than that of the pristine material (Figure S27).

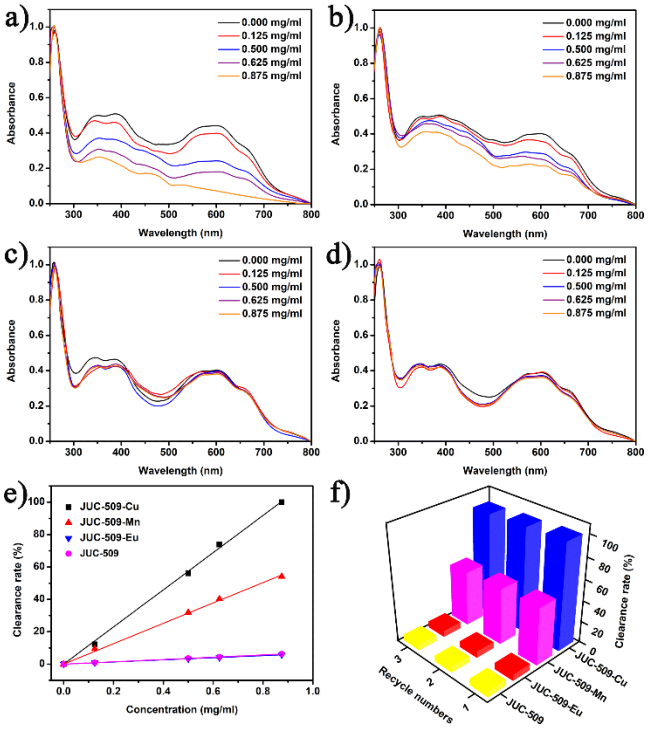

Figure 4. Adsorption spectra of JUC-509-Cu (a), JUC-509-Mn (b), JUC-509-Eu (c) and JUC-509 (d) in antioxidant secestration experiments. (e) The clearance rate based on different concentration. (f) Recyclability study of JUC-509-Cu, JUC-509-Mn, JUC-509-Eu and JUC-509.

We further explored the application of M-Salphen COFs in the removal of superoxide radical anion ($O_2^{\cdot-}$). It is well known that the overproduction of $O_2^{\cdot-}$ has been shown to contribute to tissue damage and injury.[37] Salens or Salphens with redox-active metal centers are considered as major catalytic antioxidants that catalyze the dismutation reaction of $O_2^{\cdot-}$ similar to superoxide dismutases (SODs).[38] However, the employments of traditional Salphens are strongly limited because of stability and recyclability issues. Herein, 3D-M-Salphen-COFs were chosen as effective oxygen radical removal agents due to their high surface areas, chemical stability and reusability.

Typically, $O_2^{\cdot-}$ was generated under sunlight in the presence of methionine and riboflavin, and further reacted with nitrotetrazolium blue chloride (NBT) to form a deep blue complex, which exhibited a characteristic absorption at about 560 nm in the UV-Vis spectroscopy.[39] As shown in Figure 4, 3D-M-Salphen-COFs had different activity in the elimination of superoxide radicals accompanied by the change of catalyst concentration. Among them, JUC-509-Eu had no obvious antioxidant activity, and JUC-509-Cu displayed the best performance (almost 100% clearance rate in only 0.875 mg/ml), which can be attributed to the high catalytic effect of Cu(II) ion.[40] Furthermore,

their cyclic voltammetric (CV) measurements demonstrated that JUC-509-Cu showed the best redox process in 3D-M-Salphen-COFs (Figures S33-35). As a comparison, the metal-free pristine material, JUC-509, was tested under the same condition, and showed no evidence for the removal of $O_2^{\cdot-}$ (Figure 4d and 4e), which further demonstrated the critical role of redox-active metal centers in antioxidant activity. ICP analysis of the filtrate after the reaction revealed almost no leaching of metal ions (see Section S1 in SI). PXRDs showed that the recovered solid remained crystalline and structurally intact (Figures S22-24). Most importantly, these M-Salphen COF catalysts can be readily recycled and reused at least three times without lost of activity (Figure 4f).

In conclusion, we have for the first time designed and synthesized 3D-Salphen-COFs and 3D-M-Salphen-COFs. These Salphen-based COFs showed high crystallinity, BET surface area, and chemical stability. Furthermore, the Cu(II)-Salphen COF displayed high performance in the removal of superoxide radicals and could be reused without significant activity loss. 3D Salphen-based COFs successfully prepared in this work may not only open a new pathway to create 3D functionalized COFs, but also expand the applications of COF materials in biology and medicine.

ASSOCIATED CONTENT

Supporting Information

Synthetic procedures, SEM, TEM, FTIR, solid state ^{13}C NMR, TGA, and BET plots. This material is available free of charge via the internet at http://pubs.acs.org.

AUTHOR INFORMATION

Corresponding Author

*qrfang@jlu.edu.cn

Notes

The authors declare no competing financial interests.

ACKNOWLEDGMENT

This work was supported by National Natural Science Foundation of China (21571079, 21621001, 21390394, 21571076, and 21571078), ″111″ project (B07016 and B17020), Guangdong and Zhuhai Science and Technology Department Project (2012D0501990028), and the program for JLU Science and Technology Innovative Research Team. Q.F and V.V. acknowledge the support from Thousand Talents program (China).

REFERENCES

(1) Côté, A. P.; Benin, A. I.; Ockwig, N. W.; O'Keffe, M.; Matzger, A. J.; Yaghi, O. M. *Science* **2005**, *310*, 1166.

(2) Colson, J. W.; Woll, A. R.; Mukherjee, A.; Levendorf, M. P.; Spitler, E. L.; Shields, V. B.; Spencer, M. G.; Park, J.; Dichtel, W. R. *Science* **2011,** *332*, 228.

(3) Ding, S. Y.; Wang, W. *Chem. Soc. Rev.* **2013**, *42***,** 548.

(4) Huang, N.; Wang, P.; Jiang, D. L. *Nat. Rev. Mater.* **2016,** *1*, 16068.

(5) Fang, Q. R.; Zhuang, Z. B.; Gu, S.; Kaspar, R. B.; Zheng, J.; Wang, J. H.; Qiu, S. L.; Yan, Y. S. *Nat. Commun.* **2014,** *5*, 4503.

(6) Kuhn, P.; Antonietti, M.; Thomas, A. *Angew. Chem. Int. Ed.* **2008,** *47*, 3450.

(7) Furukawa, H.; Yaghi, O. M. *J. Am. Chem. Soc.* **2009**, *131*, 8875.

(8) Wang, S.; Wang, Q.; Shao, P.; Han, Y.; Gao, X.; Ma, L.; Yuan, S.; Ma, X.; Zhou, J.; Feng, X.; Wang, B. *J. Am. Chem. Soc.* **2017,** *139*, 4258.

(9) Wan, S.; Guo, J.; Kim, J.; Ihee, H.; Jiang, D. *Angew. Chem. Int. Ed.* **2008,** *47*, 8826.

(10) Du, Y.; Yang, H.; Whiteley, J. M.; Wan, S.; Jin, Y.; Lee, S. H.; Zhang, W. *Angew. Chem. Int. Ed.* **2016,** *55*, 1737.

(11) Ding, S. Y.; Gao, J.; Wang, Q.; Zhang, Y.; Song, W. G.; Su, C. Y.; Wang, W. *J. Am. Chem. Soc.* **2011**, *133*, 19816.

(12) Li, L. H.; Feng, X. L.; Cui, X. H.; Ma, Y. X.; Ding, S. Y.; Wang, W. *J. Am. Chem. Soc.* **2017**, *139*, 6042.

(13) Han, X.; Xia, Q. C.; Huang, J. J.; Liu, Y.; Tan, C. X.; Cui, Y. *J. Am. Chem. Soc.* **2017,** *139*, 8693.

(14) Doonan, C. J.; Tranchemontagne, D. J.; Glover, T. G.; Hunt, J. R.; Yaghi, O. M. *Nat. Chem.* **2010,** *2*, 235.

(15) Kandambeth, S.; Mallick, A.; Lukose, B.; Mane, M. V.; Heine, T.; Banerjee, R. *J. Am. Chem. Soc.* **2012**, *134*, 19524.

(16) Calik, M.; Auras, F.; Salonen, L. M.; Bader, K.; Grill, I.; Handloser, M.; Medina, D. D.; Dogru, M.; Löbermann, F.; Trauner, D.; Hartschuh, A.; Bein, T. *J. Am. Chem. Soc.* **2014**, *136*, 17802.

(17) Zhou, T. Y.; Xu, S. Q.; Wen, Q.; Pang, Z. F.; Zhao, X. *J. Am. Chem. Soc.* **2014,** *136*, 15885.

(18) Peng, Y. W.; Xu, G. D.; Hu, Z. G.; Cheng, Y. D.; Chi, C. L.; Yuan, D. Q.; Cheng, H. S.; Zhao, D. *ACS Appl. Mater. Interfaces* **2016**, *8*, 18505.

(19) Sun, Q.; Aguila, B.; Perman, J.; Earl, L. D.; Abney, C. W.; Cheng, Y.; Wei, H.; Nguyen, N.; Wojtas, L.; Ma, S. Q. *J. Am. Chem. Soc.* **2017,** *139*, 2786.

(20) Jin, E. Q.; Asada, M.; Xu, Q.; Dalapati, S.; Addicoat, M. A.; Brady, M. A.; Xu H.; Nakamura, T., Heine, T.; Chen, Q. H.; Jiang, D. L. *Science* **2017,** *357*, 673.

(21) Colson, J. W.; Dichtel, W. R. *Nat. Chem.* **2013**, *5*, 453.

(22) Diercks, C. S.; Yaghi, O. M. *Science* **2017,** *355*, 923.

(23) El-Kaderi, H. M.; Hunt, J. R.; Mendoza-Cortés, J. L.; Côté, A. P.; Taylor, R. E.; O'Keffe, M.; Yaghi, O. M. *Science* **2007**, *316*, 268.

(24) Zhang, Y. B.; Su, J.; Furukawa, H.; Yun, Y. F.; Gándara, F.; Duong, A.; Zou, X. D.; Yaghi, O. M. *J. Am. Chem. Soc.* **2013**, *135*, 16336.

(25) Beaudoin, D.; Maris, T.; Wuest, J. D. *Nat. Chem.* **2013**, *5*, 830.

(26) Lin, G. Q.; Ding, H. M.; Yuan, D. Q.; Wang, B. S.; Wang, C. *J. Am. Chem. Soc.* **2016**, *138*, 3302.

(27) Yahiaoui, O.; Fitch, A. N.; Hoffmann, F.; Fröba, M.; Thomas, A.; Roeser, J. *J. Am. Chem. Soc.* **2018**, *140*, 5330.

(28) Ma, T. Q.; Kapustin, E. A.; Yin, S. X.; Liang, L.; Zhou, Z. Y.; Niu, J.; Li, L. H.; Wang, Y. Y.; Su, J.; Wang, X. G.; Wang, W. D.; Wang, W.; Sun, J. L.; Yaghi, O. M. *Science* **2018**, *361*, 48.

(29) Li, Z. L.; Li, H.; Guan, X. Y.; Tang, J. J.; Yusran, Y.; Li, Z.; Xue, M.; Fang, Q. R.; Yan, Y. S.; Valtchev, V.; Qiu, S. L. *J. Am. Chem. Soc.* **2017**, *139*, 17771.

(30) Lu, Q. Y.; Ma, Y. C.; Li, H.; Guan, X. Y.; Yusran, Y.; Xue, M.; Fang, Q. R.; Yan, Y. S.; Qiu, S. L.; Valtchev, V. *Angew. Chem. Int. Ed.* **2018**, *57*, 6042.

(31) Guan, X. Y.; Ma, Y. C.; Li, H.; Yusran, Y.; Xue, M.; Fang, Q. R.; Yan, Y. S.; Valtchev, V.; Qiu, S. L. *J. Am. Chem. Soc.* **2018**, *140*, 4494**.**

(32) Li, H.; Pan, Q. Y.; Ma, Y. C.; Guan, X. Y.; Xue, M.; Fang, Q. R.; Yan, Y. S.; Valtchev, V.; Qiu, S. L. *J. Am. Chem. Soc.* **2016**, *138*, 14783.

(33) Fang, Q. R.; Wang, J. H.; Gu, S.; Kaspar, R. B.; Zhuang, Z. B.; Zheng, J.; Guo, H. X.; Qiu, S. L.; Yan, Y. S. *J. Am. Chem. Soc.* **2015**, *137*, 8352.

(34) Fang, Q. R.; Gu, S.; Zheng, J.; Zhuang, Z. B.; Qiu, S. L.; Yan, Y. S. *Angew. Chem., Int. Ed.* **2014**, *53*, 2878.

(35) Delgado-Friedrichs, O.; O'Keeffe, M.; Yaghi, O. M. *Acta Crystallogr. Sect. A* **2006**, *62*, 350.

(36) *Materials Studio ver. 7.0*; Accelrys Inc.; San Diego, CA.

(37) Gilgun-Sherki, Y.; Melamed, E.; Offen, D. *Neuropharmacology* **2001,** *40*, 959.

(38) Day, B. J. *Thera. Focus* **2004,** *9*, 557.

(39) Riley, D. P. *Chem. Rev.* **1999,** *99*, 2573.

(40) Riley, D. P.; Weiss, R. H. *J. Am. Chem. Soc.* **1994**, *116*, 387.

TOC Graphic:

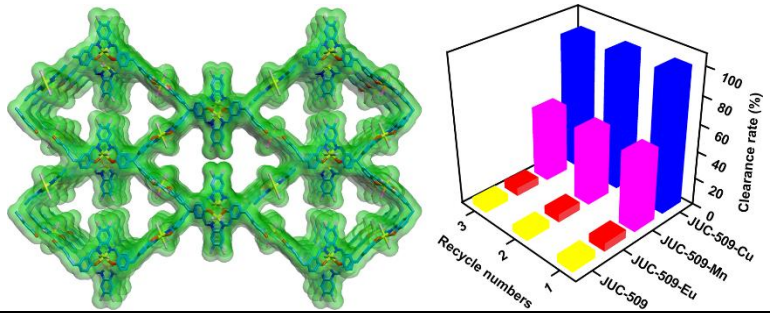
100
80
60
40
20
0
Clearance rate (%)
JUC-509-Cu
JUC-509-Mn
JUC-509-Eu
JUC-509
Recycle numbers